

## Article

# Seepage Characteristics and Influencing Factors of Weakly Consolidated Rocks in Triaxial Compression Test under Mining-Induced Stress Path

Zhiwen Chen <sup>1</sup>, Honglin Liu <sup>1,2,\*</sup> , Chengyu Zhu <sup>1</sup>, Shuqi Ma <sup>3,\*</sup>, Yinjian Hang <sup>4</sup> and Wenjie Luo <sup>1</sup><sup>1</sup> College of Geology and Mines Engineering, Xinjiang University, Urumqi 830046, China<sup>2</sup> Key Laboratory of Environmental Protection Mining for Minerals Resources at Universities of Education Department of Xinjiang Uygur Autonomous Region, Xinjiang University, Urumqi 830047, China<sup>3</sup> Key Laboratory of Transportation Tunnel Engineering, Ministry of Education, Southwest Jiaotong University, Chengdu 610031, China<sup>4</sup> Xuzhou Mining Group Co., Ltd., Xuzhou 221000, China

\* Correspondence: liuhonglin@xju.edu.cn (H.L.); masq@swjtu.edu.cn (S.M.);

Tel.: +86-1399-982-2448 (H.L.); +86-028-66365990 (S.M.)

**Abstract:** The rock of weakly consolidated coal measure strata has the characteristics of low mechanical strength and strong water sensitivity. Under the stress and seepage disturbance caused by coal seam mining, the surrounding rock structure is prone to instability, which leads to mine safety accidents and water resources loss. In order to master the mechanical response and permeability evolution law of weakly consolidated rock under the disturbance of coal seam mining, the specimens of Jurassic mudstone, sandy mudstone, and sandstone in the Ili mining area of China were collected, and a triaxial compression seepage test was carried out. A comprehensive analysis was carried out on the mineral composition and microstructure characteristics of the rock. The results show the following: (1) Compared to the constant confining pressure condition, mining-induced stress promotes the fracture development rate of weakly consolidated rocks. The ratios of strain at the yield point of mudstone, sandy mudstone, and sandstone under mining-induced stress and constant confining pressure are 0.33, 0.43, and 0.79, respectively, and the ratios of strain at the failure point were 0.48, 0.52, and 0.72, respectively. (2) Under the condition of mining-induced stress, the permeability change range and the permeability recovery rate of the three types of rocks were different, which decreased in the order of mudstone, sandy mudstone, and sandstone. (3) In the process of the triaxial compression test, there was a strong hysteresis in the permeability change of the mudstone, and the permeability and hysteresis of the three types of rocks decreased with the increase in the clay mineral content. (4) Combined with the analysis of the rock mineral composition and microstructure characteristics, it is believed that the clay minerals in the rock after water mud and swelling are the main reasons for the hysteresis of the permeability change of weakly consolidated rock, and the content of clay minerals is the main factor affecting the permeability characteristics of the weakly consolidated rock.

**Keywords:** weakly consolidated rock; permeability; mining stress; triaxial compression; clay minerals

**Citation:** Chen, Z.; Liu, H.; Zhu, C.; Ma, S.; Hang, Y.; Luo, W. Seepage Characteristics and Influencing Factors of Weakly Consolidated Rocks in Triaxial Compression Test under Mining-Induced Stress Path. *Minerals* **2022**, *12*, 1536. <https://doi.org/10.3390/min12121536>

Academic Editor: Gianvito Scaringi

Received: 13 October 2022

Accepted: 28 November 2022

Published: 29 November 2022

**Publisher's Note:** MDPI stays neutral with regard to jurisdictional claims in published maps and institutional affiliations.



**Copyright:** © 2022 by the authors. Licensee MDPI, Basel, Switzerland. This article is an open access article distributed under the terms and conditions of the Creative Commons Attribution (CC BY) license (<https://creativecommons.org/licenses/by/4.0/>).

## 1. Introduction

Weakly consolidated rocks are usually rich in clay minerals, which have low strength and high water sensitivity. When weakly consolidated rock encounters water, water molecules enter the interlayer and interparticle interfaces of the rock, resulting in the expansion of the cambium and interparticle and the destruction of the complete structure of the rock [1–3]. During the mining coal working face process, the overburden of the coal seam deforms under the disturbance of mining. The pores and fractures in weakly consolidated rock mass expand, leading to significant changes in the mechanical properties and permeability characteristics of rock mass [4–6]. After the changes in the rock

permeability characteristics, the effect of seepage water leads to the deterioration of the macroscopic mechanical strength and microstructure of weakly consolidated rock [7–9]. Therefore, it is of great significance for the safe and efficient mining of coal resources in weakly consolidated strata to study the rock seepage mechanism during coal mining in weakly consolidated strata and deeply analyze the seepage characteristics and influencing factors of weakly consolidated rock mass under mining-induced stress.

Yu et al. analyzed the change law of rock permeability with axial strain and volumetric strain in the whole stress–strain process, and deeply discussed the influence of the brittle–ductility transformation process of rock on permeability [10]. Wang et al. observed the microstructure of sandstone, analyzed its mineral content, and summarized the seepage characteristics of sandstone in triaxial compression tests under different seepage pressure conditions [11]. Wang et al. obtained the formula between the volumetric strain and permeability of rock by conducting triaxial seepage and stress coupling tests on low-permeability rock [12]. Zhang et al. studied the permeability characteristics of soft rock under the action of periodically varying osmotic pressure [13].

In order to understand the coal seam mining process, especially in the coal and rock stress path, and through the analysis of three typical mining methods, Xie et al. revealed the pressure distribution law of the front edge of the rock platform and determined the stress path characteristics of the dynamic environment of mining coal or rock, providing a basis for the laboratory testing of underground engineering rock mass. By studying the coupling mode of “stress field–fracture field–seepage field” in rock mass under different mining methods, a relationship between an increasing rate of permeability and volumetry strain was deduced [14]. Miao et al. proposed the concept of “mining-induced rock mass mechanics” on the basis of analyzing the mining dynamic characteristics of layered rock mass, which provided an effective description for studying the seepage characteristics of rock mass under mining action and the seepage characteristics of rock mass destroyed after mining. Seepage experiments on the complete stress–strain process and the non-Darcy flow of post-peak rock and broken rock were carried out [15]. Peng et al. used the triaxial rock mechanics test system to analyze the permeability change rule of sandstone in the whole stress–strain process and the porosity of rock under different confining pressures and found that both the porosity and permeability of rock decreased with an increase in the confining pressure [16]. The above research results show the basic variation law of rock permeability under different conditions. However, the seepage characteristics of weakly consolidated formation rocks under mining stress are still relatively unknown. In particular, for the Jurassic coal measure strata rocks in Northwest China, due to their short petrogenesis time, loose cementation structure, and low mechanical strength, it is necessary to further study the variation rules and influencing factors of permeability so as to ensure the safety of mine production.

On the basis of previous studies, a triaxial compression permeability test was carried out using an MTS815 testing machine to study the deformation and permeability evolution of weakly consolidated rock under mining-induced stress by collecting Jurassic strata rock samples in the Ili mining area, China. In addition, the factors influencing the seepage characteristics of weakly cemented rocks were analyzed from the aspects of microstructure and mineral composition. These analyses are helpful for determining the seepage law of weakly consolidated rock and have important significance to guide coal mining in weakly consolidated strata.

## 2. Test Principles and Methods

### 2.1. Test Rock Sample and Preparation

The weak consolidated rock core of coal seam roof 21 in the Ili mining area of China was extracted by ground drilling. After the on-site sample collection, the original rocks were first classified to remove the rock samples with more impurities, natural cracks, and weathering and to eliminate the influence of the discreteness of the samples on the test as much as possible. Then, according to the engineering rock mass test method standard,

standard columnar samples of mudstone, sandy mudstone, and sandstone were prepared with sizes of  $\varphi 50\text{mm} \times 100\text{mm}$  (diameter  $\times$  height).

2.2. Test Principle

According to the research results of Xie et al. [14], the roof rock of coal seam mainly experiences three processes in the process of coal seam mining: (1) stress of the original rock; (2) the vertical stress increases while the horizontal stress decreases until failure occurs; (3) stress recovery. In the process of caving coal mining, the peak value of vertical stress is about 2.5 times that of the stress of the original rock. The stress state of rock mass during mining is shown in Figure 1. In the process of the triaxial compression test, the axial load is the vertical stress, and the annular load (confining pressure) is the horizontal stress. The mechanical behavior of rock affected by mining is simulated by increasing the axial force of the rock sample and reducing the confining pressure. Since the permeability of the rock had to be tested in the experiment, the confining pressure could not be reduced to 0 MPa, so the minimum confining pressure was determined to be 2.0 MPa. The loading and unloading stress path of the rock under the influence of mining stress is shown in Figure 2.

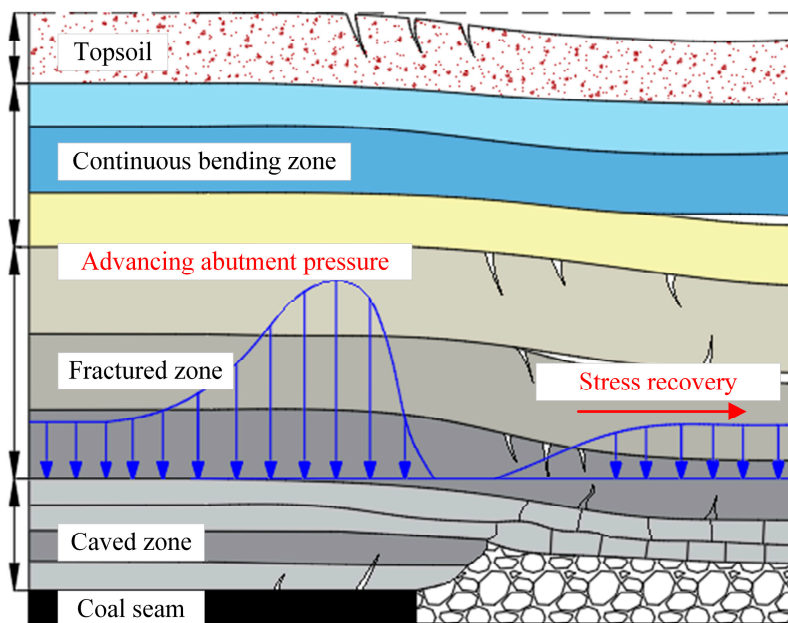


Figure 1. Stress state of surrounding rock under coal seam mining.

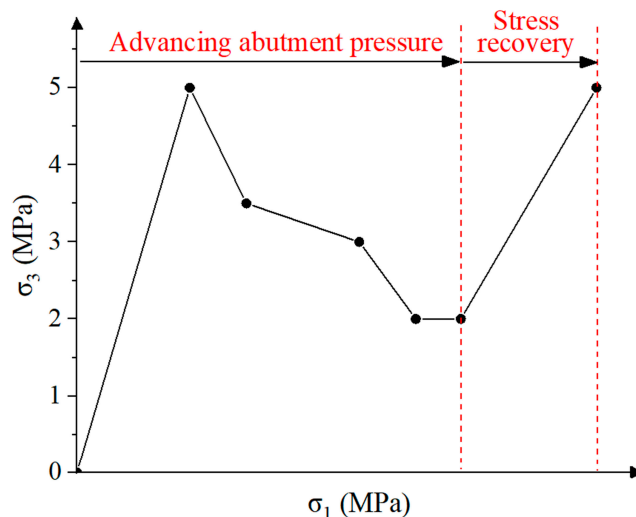


Figure 2. Loading and unloading diagram of mining stress path.

### 2.3. Test Methods

In this experiment, the permeability of rock was measured by the transient method [17], and the change rate of the pressure gradient was calculated by testing the change value of the pore pressure gradient over a certain period of time. The permeability characteristics of the rock were obtained by fitting the curve of the pressure gradient–pressure gradient change rate scatter plot. When the transient method is used, there is a stress drop phenomenon every time the pressure gradient is measured. The test equipment was the Central South University rock mechanics electro-hydraulic servo testing machine (MTS815).

The test rock samples included mudstone, sandy mudstone, and sandstone. For each type of rock sample, axial loading under constant 5.0 MPa confining pressure and mining stress path loading were adopted. After the initial surrounding rock was applied, a pressure difference of 1.0 MPa was applied, and then axial loading was carried out. The stress, strain, and permeability of the samples were monitored throughout the experiment. Note that the shape, size, processing accuracy, and loading speed of rock samples are specified by the International Society of Rock Mechanics (ISRM) [18]. The specific test process was as follows: (1) The rock specimen was wrapped around a heat-shrinkable tube and the specimen was placed in the test system. Then the water pipe, annular extensometer, and axial extensometer were installed, and the triaxial cavity was compressed. (2) First, a lower axial pressure of 0.5 MPa was applied to the axial direction and then confining pressure  $\sigma_3$  and axial pressure  $\sigma_1$  were applied to the experimental design value. (3) Pressure  $P_1$  was applied to one end of the specimen, and pressure  $P_2$  was applied to the other end to ensure that the pressure difference between the two ends ( $P_2 - P_1$ ) was 1.0 MPa. (4) The specimens were loaded axially at a loading rate of 0.003 mm/s until they were damaged. The axial stress, axial displacement, and radial displacement were monitored during the test. The sample numbers and test parameters are shown in Table 1.

**Table 1.** Rock specimen information and test program.

Experiment Number	Lithology	Confining Pressure (MPa)	Osmotic Pressure Difference (MPa)	Loading and Unloading Modes
M-01	Mudstone	5	1	Constant confining pressure
SM-01	Sandy Mudstone	5	1	
S-01	Sandstone	5	1	
M-02	Mudstone	5→2→5	1	Mining-induced stress path
SM-02	Sandy Mudstone	5→2→5	1	
S-02	Sandstone	5→2→5	1	

## 3. Test Results and Analysis

### 3.1. Stress–Strain and Permeability Relationship of Weakly Consolidated Rocks

Figure 3 shows the stress–strain–seepage curve of the three types of rock samples under constant confining pressure loading, whereas Figure 4 shows the stress–strain seepage curve of the three types of rock samples under mining-induced stress path loading. In order to characterize the permeability variation of rock samples during loading according to the triaxial compression deformation characteristics of rock, the experimental process was divided into three stages: volume compression stage (S1), yield stage (S2), and post-peak stage (S3), with the yield point and stress peak point as the boundary points [2].

Under the condition of constant confining pressure, the permeability evolution of the weakly cemented rock samples had obvious stage characteristics with the rock deformation. (1) In the volumetric compression stage (S1), the internal primary pores and cracks of the rock sample gradually closed, and the permeability of the rock specimen gradually decreased until it reached the minimum value. (2) In the yield stage (S2), the internal microfractures of the rock sample gradually developed, the permeability of the specimen began to increase, the stress gradually reached the peak strength, and the rock sample was damaged. (3) In the post-peak stage (S3), penetration cracks caused by the failure

of the specimens led to a rapid increase in permeability, and finally, the permeability of the sandstone and sandy mudstone gradually became stable, as shown in Figure 3b,c, but mudstone permeability still increases gradually and does not reach the peak, as shown in Figure 3a.

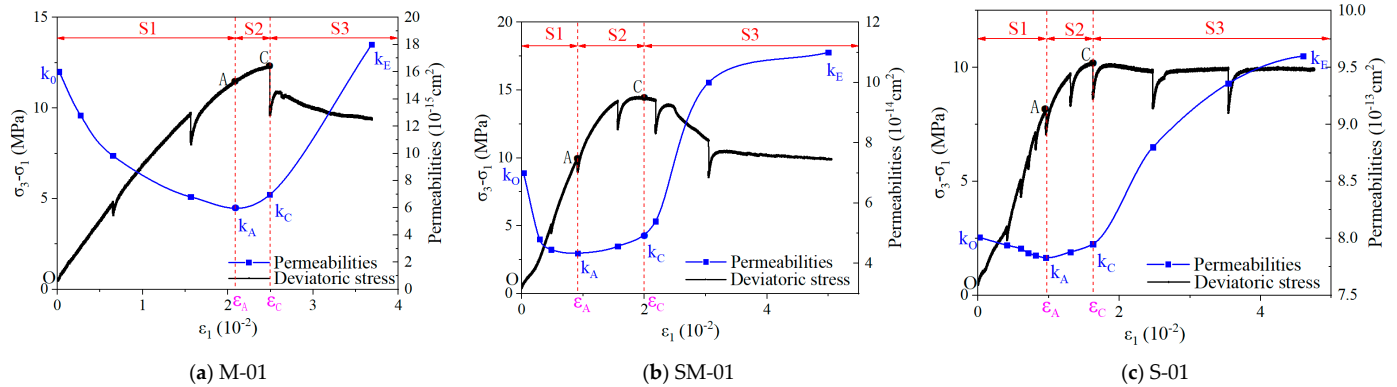


**Figure 3.** Stress-strain permeability relation curve under constant confining pressure. (a) mudstone; (b) sandy mudstone; (c) Sandstone.

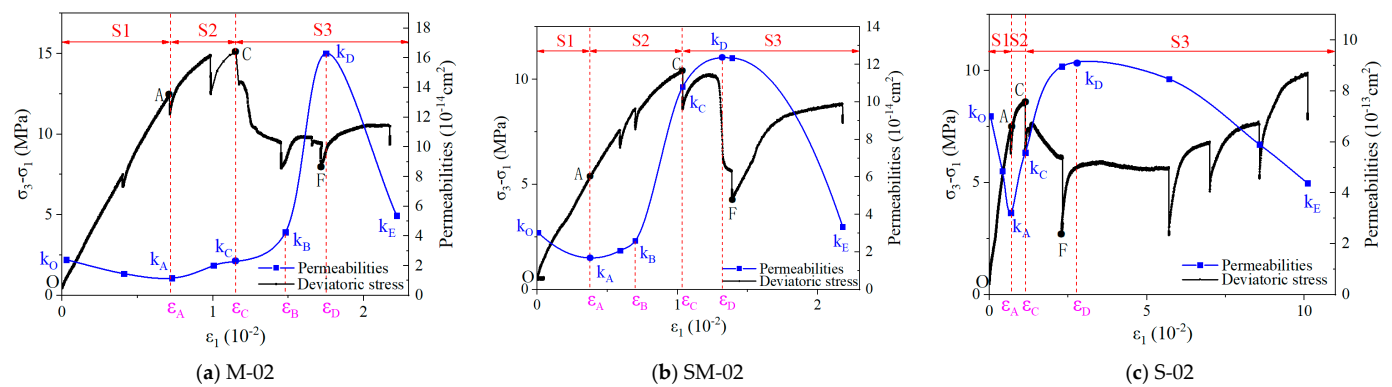


**Figure 4.** Stress-strain curve and permeability curve of rock samples under mining-induced stress path. (a) mudstone; (b) sandy mudstone; (c) Sandstone.

Compared to the seepage characteristics of the weakly consolidated rock samples under constant confining pressure, the permeability evolution under the mining-stress path had the following characteristics: (1) Under the mining stress, the strain in the volume compression stage of the weakly consolidated rock was less than 0.7%, which is relatively low compared to that under constant confining pressure. (2) The curve characteristics of the three kinds of rocks were quite different in the yield stage. At this stage, the fractures of the rock samples began to develop, and the permeability growth rate of mudstone was relatively slow, whereas those of the sandy mudstone and sandstone gradually increased. (3) The post-peak stage was mainly composed of the development process of penetrating fractures and the stress recovery process. When the rock sample reached the ultimate strength, failure occurred, and a large number of penetrating cracks were generated, which led to a rapid increase in the permeability of the rock sample. As the confining pressure of the rock samples began to increase, the volume of the rock samples began to compress gradually, and the stress of the rock samples also began to increase gradually. The internal spreading cracks and penetrating cracks of the rock samples began to close slowly, which led to a gradual decrease in the permeability of the rock samples.

In order to characterize the relationship between the stress–strain and permeability of the weakly consolidated rock, the permeability of six points, namely the initial point, yield point, mutation point, peak stress point, peak permeability point, and end point, are respectively represented by  $k_0$ ,  $k_A$ ,  $k_B$ ,  $k_C$ ,  $k_D$ , and  $k_E$ .  $\epsilon_A$ ,  $\epsilon_B$ ,  $\epsilon_C$ , and  $\epsilon_D$  are the strain

values of the corresponding points. The strain ratio at the yield point ( $R_y$ ), the strain ratio at the failure point ( $R_f$ ), and the ratio of the permeability growth rate ( $R_p$ ) of the two loading methods are shown in Table 2.

**Table 2.** Variation of strain and permeability in each stage of two loading methods.

Lithology	Constant Confining Pressure		Mining-Induced Stress Path		$R_y$	$R_f$	$R_p$
	$\varepsilon_A$ (%)	$\varepsilon_C$ (%)	$\varepsilon_A$ (%)	$\varepsilon_C$ (%)			
Mudstone	2.16	2.49	0.71	1.19	0.33	0.48	54.74
Sandy Mudstone	0.89	1.99	0.38	1.04	0.43	0.52	4.15
Sandstone	0.95	1.74	0.75	1.25	0.79	0.72	3.39

The permeability evolution characteristics under the two loading paths were compared, and the effects of mining-induced stress path loading on the permeability and strain were significant. The ratios of the strain at the yield point under mining-induced stress to the strain at the yield point under constant confining pressure ( $R_y$ ) were 0.33, 0.43, and 0.79 for the mudstone, sandy mudstone, and sandstone, and the ratios of the strain at the failure point under mining-induced stress to the strain at the failure point under constant confining pressure ( $R_f$ ) were 0.48, 0.52, and 0.72, respectively. The above results show that the mining-induced stress path loading mode promoted the fracture development rate of the weakly consolidated rock, making the rock reach the yield point faster and causing the rock sample to be more prone to failure. In the process of failure, the growth rate of the rock permeability was greatly increased. The permeability growth rates of mudstone, sandy mudstone, and sandstone under mining stress ( $R_p$ ) were 54.74 times, 4.15 times, and 3.39 times that of the rock under constant confining pressure, respectively. The permeability of the weakly consolidated rock was significantly affected by confining pressure and had a negative correlation with it.

### 3.2. Failure Morphology Analysis of Weakly Consolidated Rock Samples

The failure patterns of the mudstone, sandy mudstone, and sandstone samples under the two loading modes are shown in Figure 5. Under the condition of constant confining pressure, the failure form of the mudstone was mainly shear failure, and the specimen had many small cracks caused by the fracture, as shown in Figure 5a. The failure mode of the sandy mudstone was mainly shear failure, and the main fracture sloped upward from the bottom after testing, as shown in Figure 5b. There were two gentle shear cracks in the middle of the sandstone, and obvious plastic extrusion occurred. The integrity of the rock sample was relatively good, and the ratio of the residual strength to the peak strength was high, as shown in Figure 5c.

Under the condition of mining-induced stress, the mudstone sample had several fractures mainly characterized by tension–shear failure, as shown in Figure 5d. A shear failure fracture with an angle of  $60^\circ$  between the sandy mudstone and the horizontal plane appeared, as shown in Figure 5e. In addition to the shear failure of the sandstone, which was mainly caused by the micro-inclined fracture in the middle, there were also obvious expansion phenomena, such as plastic extrusion, as shown in Figure 5f.

By comparison, it was found that the failure degree of the mudstone was high under mining-induced stress, and the number of cracks in the whole rock sample was significantly higher than that in the mudstone sample under constant confining pressure. The failure angle of the sandy mudstone increased obviously, and the fracture ran through the whole rock sample. The plastic deformation of the sandstone was obvious, and the capacity of the circumferential expansion increased.

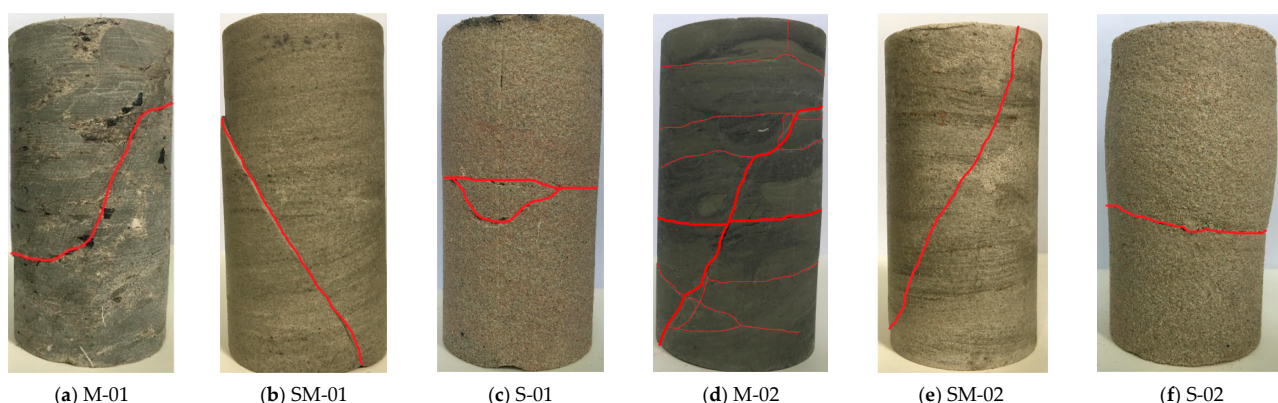


**Figure 5.** Failure characteristics of mudstone, sandy mudstone, and sandstone. (a) Constant confining pressure test of mudstone; (b) Constant confining pressure test for sandy mudstone; (c) Constant confining pressure test of sandstone; (d) Mining stress test of mudstone; (e) Mining stress test of sandy mudstone; (f) Mining stress test of sandstone.

3.3. Seepage Characteristics of Weakly Consolidated Rock under Mining-Induced Stress Path

According to the test results of the stress, strain, and permeability of the three kinds of samples, it can be seen that the loading mode of the mining-induced stress path had a significant influence on the strain–seepage characteristics of the weakly consolidated rock. In addition, the seepage characteristics of the mudstone, sandy mudstone, and sandstone under the action of mining stress were also obviously different. In order to directly reflect the seepage characteristics of the mudstone, sandy mudstone, and sandstone under mining operation, the maximum permeability growth factor (M), the magnitude of the change in permeability (N), and permeability recovery rate ( $P_r$ ) were defined to describe the permeability curve change characteristics. The maximum permeability increase factor is  $M = k_D/k_0$ ; the magnitude of the change in permeability is  $N = (k_D - k_A)/k_0$ ; the permeability recovery rate is  $P_r = (k_D - k_E)/(\epsilon_E - \epsilon_D)$ .

As can be seen in Table 3, the initial permeability ( $k_0$ ) rates of the mudstone, sandy mudstone, and sandstone were  $2.40 \times 10^{-14} \text{cm}^2$ ,  $3.03 \times 10^{-14} \text{cm}^2$ , and  $7.01 \times 10^{-13} \text{cm}^2$ , respectively. The initial permeability of the mudstone and sandy mudstone was less than  $1.00 \times 10^{-13} \text{cm}^2$ , indicating that the unfractured mudstone and sandy mudstone had lower permeability and better water isolation performance [2]. By comparison, the permeability change range and permeability recovery rate of the three types of rocks were different, and they decreased in the order of mudstone, sandy mudstone, and sandstone. The maximum permeability growth times (M) of the three samples were 6.79, 4.09, and 1.28, respectively, and the magnitude of the change in permeability (N) were 6.33, 3.40, and 0.82, respectively. This shows that the lower the initial permeability of weakly cemented rock is, the greater the permeability variation.

**Table 3.** Summary of permeability at each stage of mining stress.

Lithology	$k_0$ ( $10^{-14} \text{cm}^2$ )	$k_A$ ( $10^{-14} \text{cm}^2$ )	$k_D$ ( $10^{-13} \text{cm}^2$ )	$k_E$ ( $10^{-14} \text{cm}^2$ )	M (times)	N (times)	$P_r$ ( $10^{-12} \text{cm}^2$ )
Mudstone	2.40	1.16	1.63	5.32	6.79	6.33	23.50
Sandy Mudstone	3.03	2.10	1.24	3.25	4.09	3.40	11.18
Sandstone	70.10	32.00	8.95	43.70	1.28	0.82	5.86

In the stress recovery stage, the permeability of the mudstone and sandy mudstone could recover quickly, whereas the process of the sandstone returning to the original rock stress was relatively slow. The permeability recovery rates ( $P_r$ ) of the mudstone, sandy mudstone, and sandstone were  $2.35 \times 10^{-11} \text{cm}^2$ ,  $11.18 \times 10^{-12} \text{cm}^2$ , and  $5.86 \times 10^{-12} \text{cm}^2$ , respectively. It can be seen that the permeability recovery rates ( $k_E$ ) of the mudstone, sandy

mudstone, and sandstone decreased successively. The permeability rates of the mudstone and sandy mudstone after restoration were  $5.32 \times 10^{-14} \text{ cm}^2$  and  $3.25 \times 10^{-14} \text{ cm}^2$ , and the permeability after restoration was greater than the initial permeability. However, the permeability of the restored sandstone was  $4.37 \times 10^{-13} \text{ cm}^2$ , which is less than the initial permeability.

3.4. Permeability Hysteresis Analysis of Weakly Consolidated Rock under Mining-Induced Stress Path

It can be seen in Figure 4 that the permeability curves of the mudstone and sandy mudstone first experienced a period of slow growth, whereas the sandstone did not have this stage. The permeability surge point of the mudstone was after the stress peak point. The permeability spike point of the sandy mudstone was before the stress peak. The permeability spike point of the sandstone basically coincided with the yield point before the stress peak. This shows that the permeability of the mudstone and sandy mudstone lagged behind the fracture state of the rock. According to the crack strain model [19,20], the permeability of the rock is mainly affected by the degree of crack development. For rock specimens under triaxial compression, the volumetric strain  $\epsilon_v$  can be expressed as:

$$\epsilon_v = \epsilon_1 + 2\epsilon_3 \tag{1}$$

where  $\epsilon_1$  and  $\epsilon_3$  are the axial and annular strains of rock, respectively.

The volume strain can be divided into two parts: one is the volume strain  $\epsilon_{cv}$  caused by crack closure, initiation, opening, and penetration during loading. The other part is the elastic volumetric strain  $\epsilon_{ev}$  at the same stress level. The crack volumetric strain can be obtained by subtracting the elastic volumetric strain from the total volumetric strain, and the calculation formula is:

$$\epsilon_{cv} = \epsilon_v - \frac{(1 - 2\nu)(\sigma_1 + 2\sigma_3)}{E} \tag{2}$$

where E is the elastic modulus and the average slope of the stress–strain curve is taken. The elastic modulus of mudstone, sandy mudstone, and sandstone is 1.49 GPa, 1.08 GPa, and 0.83 GPa, respectively;  $\nu$  is Poisson’s ratio,  $\nu = \epsilon_3/\epsilon_1$ ;  $\sigma_1$  and  $\sigma_3$  are the axial and lateral stresses, respectively.

Figure 6 shows the volumetric strain curves of the fractures in the mudstone, sandy mudstone, and sandstone under mining-induced stress. It can be seen that the fit degree of the crack volume–strain curve and the permeability curves of the mudstone, sandy mudstone, and sandstone increased successively. The permeability curve of the mudstone lagged behind the volume–strain curve of the rock crack, indicating that the permeability of the mudstone did not increase rapidly after the development of cracks, and there was a strong lag in the change of mudstone permeability.

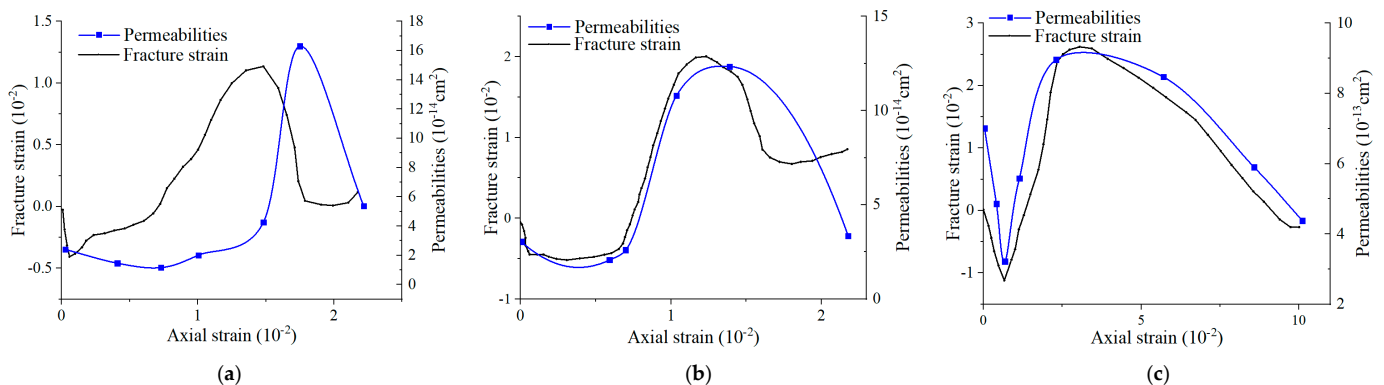
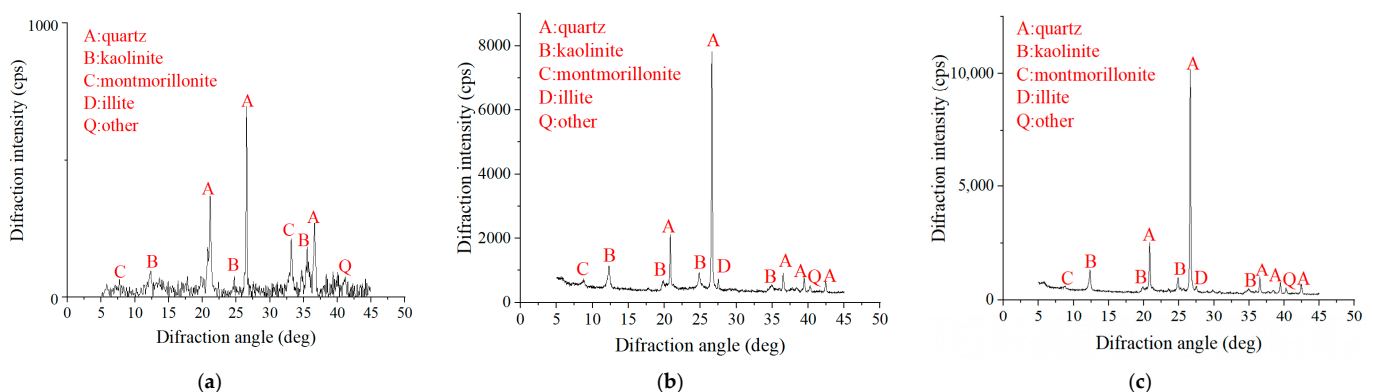


Figure 6. Volumetric strain and permeability curves of rock fracture under mining-induced stress path. (a) mudstone fracture strain; (b) Fracture strain of sandy mudstone; (c) sandstone fracture strain.

#### 4. Analysis of Influence Factors on Seepage Characteristics of Weakly Consolidated Rocks

The permeability changes of the mudstone, sandy mudstone, and sandstone were different at each stage of the mining stress, and there was a strong lag in the mudstone. In order to explore the factors affecting the permeability characteristics of the weakly consolidated rocks, X-ray diffraction (XRD) and scanning electron microscopy (SEM) were used to further study the mineral composition and microstructure of the three kinds of rocks.

An XRD test was used to analyze the mineral components of the weakly consolidated mudstone, sandy mudstone, and sandstone, and the diffraction pattern is shown in Figure 7. The XRD test results show that the mudstone was rich in clay minerals, such as kaolinite, montmorillonite, and illite, whereas the sandy mudstone and sandstone were dominated by kaolinite and illite. The contents of clay minerals in the three samples are shown in Table 4. The proportions of clay minerals in the mudstone, sandy mudstone, and sandstone were 71%, 36%, and 25%, respectively. The clay minerals of the mudstone were mainly composed of kaolinite, an illite/montmorillonite mixed layer, and illite, accounting for 30.53%, 34.79%, and 5.68% of the total clay minerals, respectively. Kaolinite was the main clay mineral in the sandy mudstone, and its clay mineral content was 24.84%. Kaolinite was the main clay mineral in the sandstone, and its content was 17.25%. The clay mineral content of the mudstone was 1.97 times that of the sandy mudstone and 2.84 times that of the sandstone. The clay mineral content of the mudstone, sandy mudstone, and sandstone decreased successively, whereas the permeability increased gradually, indicating that the permeability and clay mineral contents had a negative correlation.



**Figure 7.** X-ray diffraction patterns of specimens. (a) Diffraction results of mudstone; (b) Diffraction results of sandy mudstone; (c) Diffraction results of sandstone.

**Table 4.** Results of composition analysis in specimens by X-ray.

Lithology	Quartz (%)	Kaolin (%)	Illite/Smectite Formation (%)	Illite (%)	Other (%)	Clay Minerals (%)
Mudstone	29	30.53	34.79	5.68	0	71
Sandy mudstone	60	24.84	6.84	4.32	4	36
Sandstone	70	17.25	4.5	3.25	5	25

The SEM results of the weakly consolidated mudstone, sandy mudstone, and sandstone are shown in Figure 8. There were certain primary pores in the weakly cemented rocks. The structure of the rock mineral particles was loose and the outline is clearly visible. The clastic fillings were filled in the pore structure, and the cementation type was mainly pore-filling cementation. Under the magnification of 2000 times, it was observed that the internal structure of the sandstone was loose and there were many pores. The particle size of the sandstone was large, mainly distributed between 20 and 75  $\mu\text{m}$ , and the particles were disordered. It can be clearly seen that the flocculent montmorillonite was distributed on the particle surface and the bulk kaolinite was filled in the pores. Compared to the

sandstone, the internal structure of the sandy mudstone was closer, with a small number of pores, and the particle size was mainly distributed between 8 and 15  $\mu\text{m}$ . The internal structure of the mudstone was dense, but there were also a few tiny pores, and the particle size was small, mainly distributed between 5 and 12  $\mu\text{m}$ . When magnified to 8000 times, it was observed that the maximum pore spacing of the sandstone was 30.02  $\mu\text{m}$ , a small amount of a flocculent illite/montmorillonite mixed layer filled in the pores, and the particle cementation degree was poor. The pore spacing of the sandy mudstone was 15–23  $\mu\text{m}$ , and there was a lot of flocculent illite/montmorillonite mixed layer filling between the pores. The pore spacing of the mudstone was 21.78  $\mu\text{m}$ , and the pores were small. There was also a lot of flocculent illite/montmorillonite mixed layer and flake illite on the surface of the rock sample, and the particle cementation degree was good.

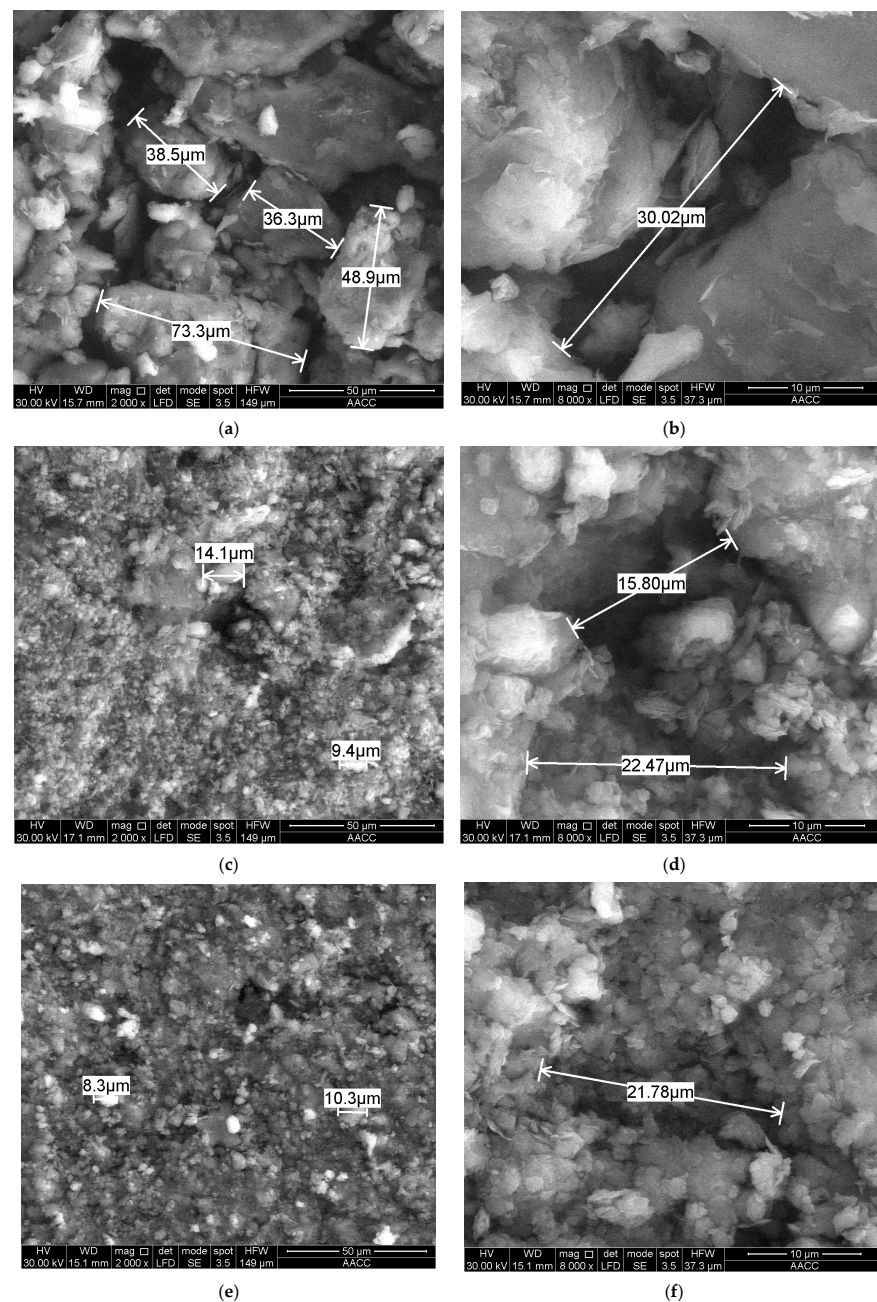


**Figure 8.** Scanning electron microscopy of rock under natural moisture content. (a) Sandstone (2000 $\times$  magnification); (b) Sandstone (8000 $\times$  magnification); (c) Sandy mudstone (2000 $\times$  magnification); (d) Sandy mudstone (8000 $\times$  magnification); (e) Mudstone (2000 $\times$  magnification); (f) Mudstone (8000 $\times$  magnification).

The content of clay minerals in the sandstone was small, its structure was loose, and it had many internal pores. However, the mudstone had high clay mineral content and a dense internal structure, which may be the main factors leading to the low permeability and strong water isolation performance of mudstone. Due to the loose structure and voids in the rock samples, the rock was compressed after the triaxial compression test began, resulting in the initial permeability of most rock samples being more than twice the minimum permeability. Under the mining-induced stress path, the pore structure of the mudstone and sandy mudstone first transformed from the compact state to the loose state, and gradually recovered after the stress recovery. However, the permeability of the rock sample after the stress recovery was greater than the initial permeability because the integrity of the rock sample was destroyed by the penetrating cracks. There were many pores and large pore spacing in the sandstone, and the decrease in the pore spacing in the sandstone after stress recovery led to the final permeability being less than the initial permeability.

Due to the high clay content of the rock samples, they easily reacted with water. In order to study the change characteristics of the microstructure of the rock after water exposure, scanning electron microscopy (SEM) was used to study the microstructure of the saturated water samples.

It can be observed in Figure 9 that the surface of the sandy mudstone was very uneven under the condition of the saturated water, and some large particles (20–40  $\mu\text{m}$ ) were exposed. The internal structure was relatively close, but there were many pores. The larger pores had less filling, and the smaller pores had more filling between the particles. The surface of the mudstone was not very smooth in the saturated state, and some large particles (10–20  $\mu\text{m}$ ) were exposed. Compared to the mudstone samples in the natural state, the internal structure was relatively compact, a large amount of filling existed between the pores and the particles, and there was no pore larger than 20  $\mu\text{m}$  at 8000 times magnification. By comparing the SEM images of the natural state and the saturated state, the following was found: (1) The white flocculent montmorillonite expanded in the saturated state of the mudstone and sandy mudstone. (2) The surface of the mudstone and sandy mudstone was rough under saturated conditions, whereas the surface was relatively smooth and compact under natural conditions. (3) In the saturated state, the clay minerals of the mudstone and sandy mudstone moved with the water flow and filled into the smaller fractures.

Because clay minerals exhibit obvious expansion and slime characteristics when encountering water, clay minerals will disperse and migrate under the action of water [21]. Combined with weak cemented rock in the process of the triaxial compression test, the factors affecting the permeability lag are as follows: (1) The volume compression stage, which gradually occurred in the sample of natural pore closure, did not yet form a new crack. The second infiltration of water caused the clay minerals to expand, and the mud, after the expansion of the clay minerals filled in the primary pores. As a result, the permeability gradually decreased until the minimum permeability was reached. The higher the clay mineral content, the longer the clay mineral expansion and the mud process lasts. (2) When entering the yield stage, fractures developed gradually, leading to a gradual increase in permeability. However, the development of cracks caused the clay minerals to make contact with the water more fully, which made the clay minerals expand and migrate, thus blocking the seepage channel. Therefore, in the yield stage of mudstone and sandy mudstone, the permeability first increased steadily, and then increased rapidly with the rock failure to a certain extent, whereas the sandstone did not have a stable growth process.

In conclusion, in the triaxial compression permeability test, the weakly cemented rock mainly shows the following two characteristics: on the one hand, the mechanical strength of the rock is greatly reduced after water immersion; on the other hand, with the development of cracks, the interaction between clay minerals and water becomes more sufficient, which leads to the hysteresis of rock permeability curve and affects the seepage characteristics of the rock. The content of clay minerals determines the degree of hysteresis and the seepage characteristics of the rock mass.

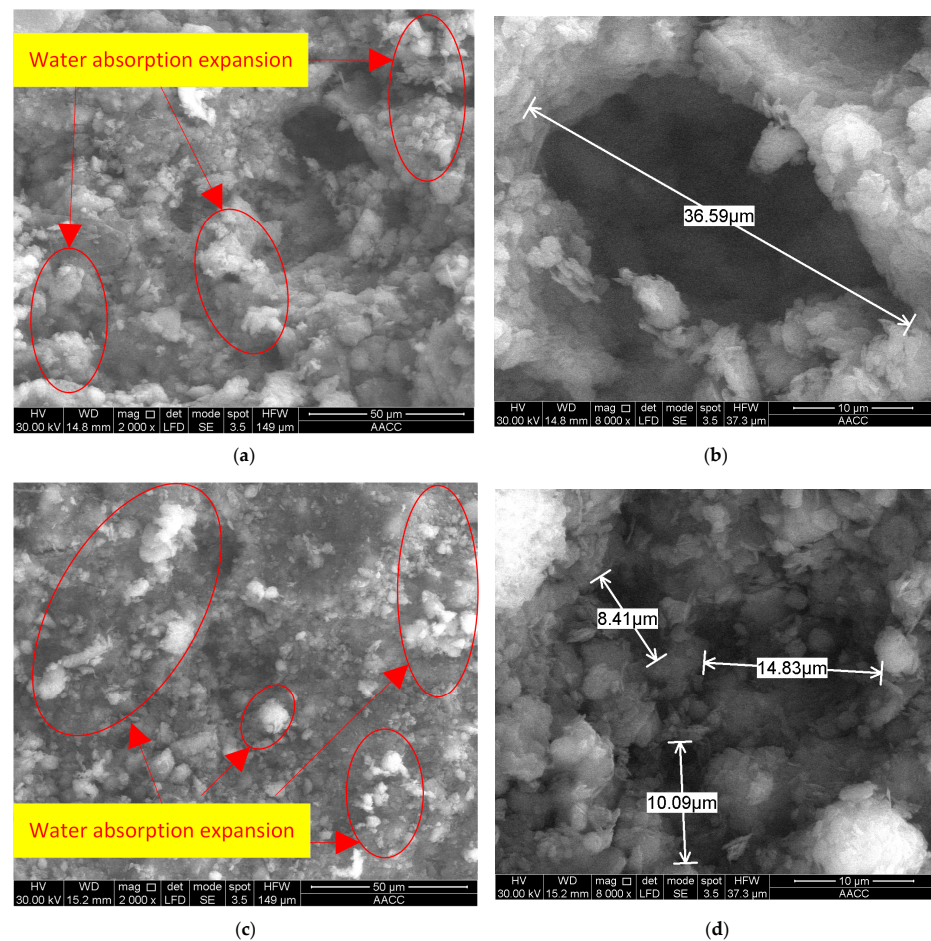


**Figure 9.** SEM images of mudstone and sandstone in saturated water state. (a) Sandy mudstone (2000× magnification); (b) Sandy mudstone (8000× magnification); (c) Mudstone (2000× magnification); (d) Mudstone (8000× magnification).

## 5. Conclusions

In this study, a triaxial compression seepage test under constant confining pressure and mining-induced stress was carried out on weakly consolidated rock. Through testing the deformation characteristics and permeability law of mudstone, sandy mudstone, and sandstone combined with XRD and scanning electron microscopy to analyze the mineral composition and microstructure characteristics of weakly consolidated rock, the main conclusions are as follows:

- (1) Compared to the constant confining pressure condition, mining stress promotes the fracture development rate of rock, and the strain at the yield point and peak point of the rock is greatly reduced. The ratios of the strain at the yield point under mining stress and constant confining pressure loading were 0.33, 0.43, and 0.79 for the mudstone, sandy mudstone, and sandstone, and the ratios of the strain at the failure point under mining stress and constant confining pressure loading were 0.48, 0.52, and 0.72, respectively. The ratios of the permeability growth rate under mining stress to that under constant confining pressure were 54.74, 4.15, and 3.39, respectively.
- (2) Under the condition of mining-induced stress, the permeability change amplitude and the permeability recovery rate of the three types of rocks were different. The permeability recovery rates of the mudstone, sandy mudstone, and sandstone were  $2.35 \times 10^{-11} \text{cm}^2$ ,  $11.18 \times 10^{-12} \text{cm}^2$ , and  $5.86 \times 10^{-12} \text{cm}^2$ , respectively, and the maximum variation ranges of permeability were 6.79 times, 4.09 times, and 1.28 times, respectively.

- (3) The proportions of clay minerals in the mudstone, sandy mudstone, and sandstone were 71%, 36%, and 25%, respectively, and the clay minerals in the mudstone were mainly an illite/montmorillonite mixed layer. Kaolinite was the main clay mineral in sandy mudstone and sandstone. Combined with the permeability curve of the mining-induced stress path, the permeability of the weakly consolidated rock samples was negatively correlated with the clay mineral content.
- (4) Clay minerals have the characteristics of swelling, slime, and migration after encountering water, which is the main reason for the hysteresis of the rock permeability curve change. The content of clay minerals is the main factor affecting the seepage characteristics of weakly consolidated rock, and the content of clay minerals also determines the hysteresis of weakly consolidated rock.

**Author Contributions:** Conceptualization, Z.C., H.L. and S.M.; methodology, H.L., Z.C. and S.M.; software, Z.C. and H.L.; validation, Z.C., C.Z. and Y.H.; investigation, Z.C., Y.H. and W.L.; data curation, Z.C. and H.L.; writing—original draft preparation, Z.C. and S.M.; writing—review and editing, Z.C., H.L. and S.M. All authors have read and agreed to the published version of the manuscript.

**Funding:** This research was funded by the National Natural Science Foundation of China, grant number 51964043 and U1903216; the Natural Science Foundation of Xinjiang Uygur Autonomous Region 2019D01C023 and 2022D02E22; and the National College Student Innovation Project, grant number 202210755007.

**Data Availability Statement:** The research data used to support the findings of this study are currently under embargo while the research findings are commercialized. Requests for data, 12 months after publication of this article, will be considered by the corresponding author.

**Acknowledgments:** The author would like to thank H.L. for her continuous support in data and writing of the paper.

**Conflicts of Interest:** The authors declare no conflict of interest.

## References

1. Guo, S.R.; Pu, H.; Yang, M.S.; Liu, D.; Sha, Z.H.; Xu, J.C. Study of the Influence of Clay Minerals on the Mechanical and Percolation Properties of Weakly Cemented Rocks. *J. Geofluids* **2022**, *2022*, 1712740. [[CrossRef](#)]
2. Fan, G.W.; Chen, M.W.; Zhang, D.S.; Wang, Z.; Zhang, S.Z.; Zhang, C.G.; Li, Q.Z.; Cao, B.B. Experimental Study on the Permeability of Weakly Cemented Rock under Different Stress States in Triaxial Compression Tests. *J. Geofluids* **2018**, *2018*, 9035654. [[CrossRef](#)]
3. Ho, T.A.; Criscenti, L.J.; Greathouse, J.A. Revealing Transition States during the Hydration of Clay Minerals. *J. Phys. Chem. Lett.* **2019**, *10*, 3704–3709. [[CrossRef](#)] [[PubMed](#)]
4. Dessouki, M.; Hathon, L.; Myers, M. Permeability and Porosity Modelling for Resedimented Mudrocks—Applications for Compaction Dominated Mudrock Systems. *Mar. Pet. Geol.* **2021**, *128*, 104945. [[CrossRef](#)]
5. Harsh, B.V.; Brandon, D. Porosity-Permeability Relationships in Mudstone from Pore-Scale Fluid Flow Simulations using the Lattice Boltzmann Method. *Water Resour. Res.* **2019**, *55*, 7060–7071.
6. Reece, J.S.; Flemings, P.B.; Dugan, B.; Long, H.; Germaine, J.T. Permeability-porosity relationships of shallow mudstones in the Ursa Basin; northern deepwater Gulf of Mexico. *J. Geophys. Research. Solid Earth* **2012**, *117*. [[CrossRef](#)]
7. Wang, Z.K.; Li, W.P.; Chen, J.F. Application of Various Nonlinear Models to Predict the Uniaxial Compressive Strength of Weakly Cemented Jurassic Rocks. *Nat. Resour. Res.* **2022**, *31*, 371–384. [[CrossRef](#)]
8. Liu, H.L.; Zhang, D.S.; Zhao, H.C.; Chi, M.B.; Yu, W. Behavior of Weakly Cemented Rock with Different Moisture Contents under Various Tri-Axial Loading States. *Energies* **2019**, *12*, 1563. [[CrossRef](#)]
9. Shi, L.; Zeng, Z.J.; Bai, B.; Li, X.C. Effect of the intermediate principal stress on the evolution of mudstone permeability under true triaxial compression. *Greenh. Gases Sci. Technol.* **2018**, *8*, 37–50. [[CrossRef](#)]
10. Yu, J.; Li, H.; Chen, X.; Cai, Y.; Wu, N.; Mu, K. Triaxial experimental study of associated permeability-deformation of sandstone under hydro-mechanical coupling. *Chin. J. Rock Mech. Eng.* **2013**, *32*, 1203–1213.
11. Wang, H.L.; Xu, W.Y.; Jia, C.J.; Cai, M.; Meng, Q.X. Experimental Research on Permeability Evolution with Microcrack Development in Sandstone under Different Fluid Pressures. *J. Geotech. Geoenviron. Eng.* **2016**, *142*, 04016014. [[CrossRef](#)]
12. Wang, W.; Xu, W.Y.; Wang, R.B. Permeability of dense rock under triaxial compression. *J. Chinese Journal of Rock Mechanics and Engineering* **2015**, *34*, 40–47.
13. Zhang, Z.H.; Sun, Q.C.; Li, D.Z. Experimental study on permeability characteristics of red sandstone under cyclic seepage pressures. *Chin. J. Geotech. Eng.* **2015**, *5*, 937–945.

14. Xie, H.P.; Zhou, H.W.; Liu, J.F. Mining-induced mechanical behavior in coal seams under different mining layouts. *J. China Coal Soc.* **2011**, *36*, 1067–1074.
15. Miao, X.X. Review of research on mechanical behaviors of mining rock mass and its related engineering technological innovation progress. *Chin. J. Rock Mech. Eng.* **2010**, *29*, 1988–1998.
16. Peng, S.P.; Meng, Z.P.; Wang, H. Testing study on pore ration and permeability of sandstone under different confining pressures. *Chin. J. Rock Mech. Eng.* **2003**, *22*, 742–746.
17. Zhang, P.S.; Zhao, C.Y.; Hou, J.Q. Experimental study on seepage characteristics of deep sandstone under high temperature and different hydraulic pressures. *Chin. J. Rock Mech. Eng.* **2020**, *39*, 1957–1974.
18. *ASTM D4543-01*; Standard Practices for Preparing Rock Core Specimens and Determining Dimensional and Shape Tolerances. ASTM International: West Conshohocken, PA, USA, 2001.
19. Brace, W.F.; Paulding, B.W.; Scholz, C. Dilatancy in the fracture of crystalline rocks. *J. Geophys. Res.* **1966**, *71*, 3939–3953. [[CrossRef](#)]
20. Martin, C.D. The Strength of Massive Lac du Bonnet Granite around Underground Openings. Ph.D. Thesis, University of Manitoba, Winnipeg, MB, Canada, 1993.
21. Zhang, W.; Zhang, D.X.; Zhao, J.L. Experimental investigation of water sensitivity effects on microscale mechanical behavior of shale. *Int. J. Rock Mech. Min. Sci.* **2021**, *145*, 104837. [[CrossRef](#)]